Review article

Deep learning-based fault diagnosis and Electrochemical Impedance Spectroscopy frequency selection method for Proton Exchange Membrane Fuel Cell ☆

Jianfeng Lv [a], Zhongliang Yu [b,a], Guanghui Sun [a], Jianxing Liu [a,*]

[a] Department of Control Science and Engineering, Harbin Institute of Technology, Harbin, 150001, PR China
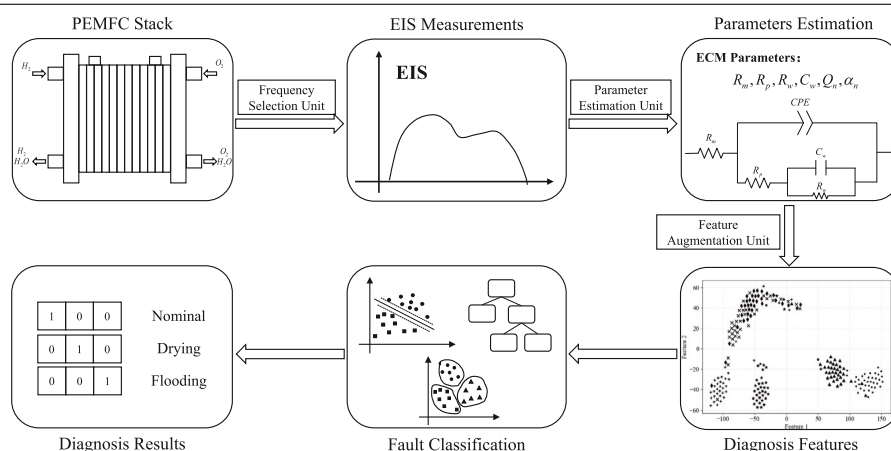[b] The College of Automation, Chongqing University, Chongqing, 400044, PR China

HIGHLIGHTS

- EIS-based fault diagnosis method is proposed to address the fault diagnosis of PEMFC.
- Frequency selection unit is proposed to find redundant frequencies in EIS.
- Discrete loss function is used to avoid the duplicate selection of frequencies.

GRAPHICAL ABSTRACT

ARTICLE INFO

ABSTRACT

Electrochemical Impedance Spectroscopy (EIS) serves as a valuable tool for analyzing the health of Proton Exchange Membrane Fuel Cell (PEMFC). However, the practical application of EIS-based fault diagnosis algorithms continues to face challenges, including time-consuming EIS measurements, inefficient Equivalent Circuit Model (ECM) parameter estimation, and limited generalization capability of fault diagnosis models. To enhance the utility of the EIS-based fault diagnosis methods, this paper develops a new deep-learning-based PEMFC fault diagnosis framework, along with a frequency selection method. Specifically, a Parameter Estimation Unit (PEU) is introduced to derive the ECM parameters directly from EIS measurements. A Frequency Selection Unit (FSU) based on the Gumbel-Softmax trick is proposed to enable the identification of the optimal frequency solution to maximize fault diagnosis performance with a predetermined number of measured frequency points. Furthermore, a Feature Augmentation Unit (FAU) is proposed to generate robust diagnosis features based on ECM parameters, thus reducing the influence of non-fault operations on fault

diagnosis results. Experiments based on real EIS data demonstrate the effectiveness of the proposed algorithm. With these innovations, the proposed framework could significantly improve the efficiency and accuracy of fault diagnosis in PEMFC.

1. Introduction

Proton exchange membrane fuel cell (PEMFC), as a clean and high-power density renewable energy source, is well-applied in various fields, including rail transportation, intelligent manufacturing, and aerospace [1]. However, reliability and durability are still challenging problems that impede the large-scale commercialization of PEMFC system [2]. PEMFC commonly utilize an electrolyte membrane to facilitate the transport of hydrogen protons from the anode to the cathode. Proper hydration of these membranes is essential to achieve optimal performance and extend their operational lifespan. Inadequate hydration results in reduced proton conductivity, leading to increased resistive losses, diminished net power output, and the development of local hotspots. Conversely, excessive moisture within the membrane or the gas diffusion layer, commonly referred to as flooding, also hampers FC performance. This is primarily due to water obstructing the flow channels, porous electrodes, and backing layers. Therefore, effective water management is recognized as a critical factor for enhancing the performance of PEMFC [3].

An efficient fault diagnosis framework is deemed essential within the realm of Prognostic and Health Management (PHM) systems, particularly for the purpose of diagnosing faults such as flooding and membrane drying [4]. The health state of a PEMFC can be represented by various measurements, with electrochemical impedance spectroscopy (EIS) being a credible signal for monitoring the internal characteristics of PEMFC without affecting its operational state [4,5]. Therefore, EIS-based fault diagnosis methods have been extensively investigated in recent years by numerous researchers [5–7].

The EIS-based diagnosis method usually consists of three steps: (i) obtaining the impedance of the PEMFC at various test points within the specified frequency range. (ii) Estimating the parameters of equivalent circuit model (ECM) based on EIS measurements and (iii) using the parameters of ECM to predict the health states of PEMFC. In general, the classification methods could output the diagnosis results efficiently in step (iii), but steps (i) and (ii) remain time-consuming. The measurement of the EIS always takes several minutes [8], and the traditional optimization-based algorithms estimate the ECM parameter with an iteration paradigm, which is also inefficient. Therefore, an effective diagnosis framework is necessary for the application of EIS-based methods.

The efficiency of the diagnosis algorithms could be improved from two perspectives. On the one hand, some methods attempt to speed up the measurement of the EIS data. Katayama and Kogoshi [9] proposed to perturb the PEMFC system by a single that consists of multiple frequency sinusoidal waves, which reduced the measurement time of EIS while simultaneously decreasing the amplitude of the excitation signal. Hong et al. [10] introduced parallel DC/DC converters to realize the sine wave disturbance signal injection and impedance measurement at high frequency. Lu et al. [5] utilized the current pulse injection circuit to disturb the PEMFC system and obtained the EIS by continuous wavelet transform and the maximum likelihood estimation method. Although these methods could reduce the time required for EIS measurement, complex algorithms are also required by these methods to obtain the parameters of the frequency spectrum, the computational complexity and hardware cost of these approaches need to be considered.

Another paradigm to cut down the diagnosis time-consumption is to optimize the fault diagnosis framework from a global view. These methods attempt to reduce the number of frequency points that need to be measured in EIS data while maintaining fault diagnosis

accuracy. Xiao et al. [11] proposed an EIS measurement optimization method to separate the feature frequency bands, removed the redundant frequency band, and diagnosis PEMFC faults by impedances in the selected frequency points. Najafi et al. [12] employed the feature selection procedure to find the best combination of EIS frequency points, which could obtain good fault diagnosis results and requires the lowest EIS testing time. Ma et al. [13] utilized the combination weighting method to select the optimal frequency points for fault diagnosis from the view of objective and subjective. These algorithms find the rough range of redundant frequency points by qualitative analysis and lack quantitative analysis of individual frequency point. In addition, these methods do not establish a direct mapping relationship from EIS data to fault diagnosis results, and the potential of fault diagnosis algorithms is not fully exploited, hence, the accuracy of fault diagnosis results is limited.

To improve the efficiency of the EIS-based fault diagnosis framework, a deep learning-based PEMFC fault prognosis framework, accompanied by a corresponding frequency selection method, is proposed in this work. Firstly, a parameter estimation unit (PEU) is developed to uncover the inherent relationship between EIS data and ECM parameters. Secondly, a frequency selection unit (FSU) is designed based on the Gumbel-Softmax trick [14], which could identify redundant frequency points in the EIS data and maximize fault diagnosis performance while adhering to a predetermined number of measured frequency points. Specifically, a discrete loss function is proposed in FSU to avoid the selection of duplicate frequencies. Finally, a feature augmentation unit (FAU) is introduced to transform the ECM parameters into robust diagnosis features, which could enhance the robustness and generalizability of the proposed framework. These generated diagnosis features are fed into a simple classifier to yield diagnosis results, and the basic framework of the proposed method is shown in Fig. 1. The performance of the diagnosis framework is evaluated using EIS data obtained from a commercial PEMFC, and the effectiveness of our proposed method is demonstrated through a series of diverse experiments.

2. Fault diagnosis method

2.1. Deep learning based fault diagnosis

The proposed method follow the basic procedure of traditional EIS-based fault diagnosis frameworks, which analyze the EIS data by ECM and utilized the parameters of ECM impedance function as the fault diagnosis features to output diagnosis results. However, unlike the traditional approaches, we discard the previous practice of estimating ECM parameters from EIS data with optimization algorithms and instead utilize neural networks to generate diagnosis results with end-to-end manner. The proposed framework comprises two phases: the offline training phase and the online testing phase. The offline training phase, depicted in Fig. 2(a), consists of two steps. Firstly, the FSU and PEU are trained jointly with a large-scale simulated EIS dataset. The PEU could predict the ECM parameters from corresponding EIS measurements, and FSU is utilized to find the redundant frequency points in EIS that useless for ECM parameter estimation and fault diagnosis. The MSE loss and proposed discrete loss are used to restrict the training direction of the networks. Secondly, the FAU is trained by actual EIS measurements with the contrastive learning paradigm. The trained PEU and FSU are utilized to generate ECM parameters from the actual EIS measurements, and these parameters will be fed into FAU to generate reliable features. Notice that only the parameters of the FAU are trained during second step.

The optimal frequency selection solution could be derived from the parameters of the trained FSU. And only a predefined number of
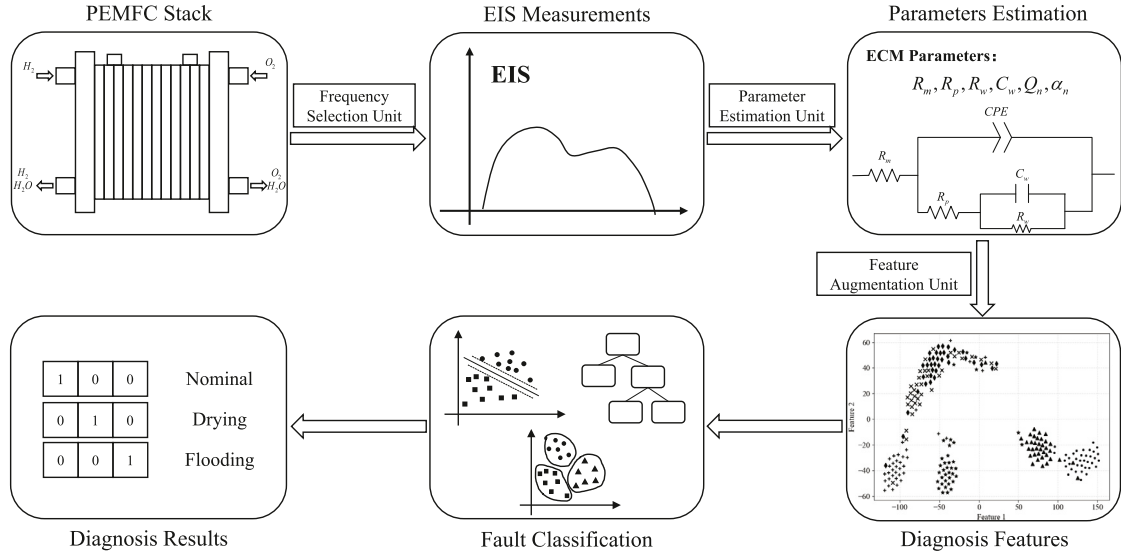
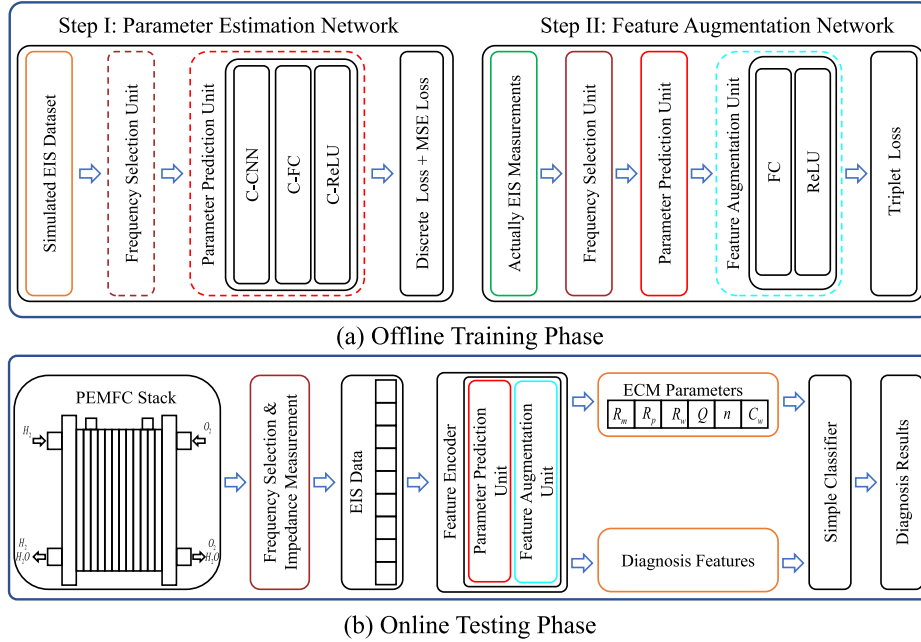**Fig. 1.** The overview of the EIS-based fault diagnosis method.

Fig. 2. The overview of the proposed framework.

frequency points need to be measured in the online testing phase, which reduces the time-consumption of EIS measurement. The structure of the online testing phase is shown in Fig. 2(b). The acquired impedances are processed by the proposed feature encoder to generate diagnosis features and corresponding ECM parameters. These features are then used to output diagnosis results with a simple classifier. The proposed method effectively explores the combination of different frequency points in EIS, and finds the best combination solution for fault diagnosis. These advantages make the proposed method more friendly to real applications.

2.2. Generation of simulated EIS dataset

The deep learning models require a large amount of data to drive the training process of the network, but it is expensive to collect such scale EIS data in the real world. Recently, knowledge-based deep learning methods have received lots of attention and are well-accepted

in many fields [15]. These methods generate simulated datasets based on prior knowledge, and these datasets could help the neural network to accomplish the specific task. Inspired by this model, he measured EIS data and prior knowledge about PEMFC are integrated to generate a large amount of simulated EIS data and use the generated data to enable the training of the PEU and FSU.

During the EIS dataset generation process, the actual measured EIS data will be analyzed by ECM first. The ECM parameters of measured EIS data could be obtained by model fitting results, and the corresponding noise of each measured EIS sample also could be estimated. Based on generated ECM parameters and noises, the distribution of ECM parameter $\mathcal{F}(P)$ and the EIS sample noise $\mathcal{F}(N)$ could be summarized. After that, the new ECM parameters could be yielded randomly, and corresponding EIS data also could be calculated by impedance function. Finally, the new noises could be produced based on $\mathcal{F}(N)$, and the EIS simulated dataset can be obtained by adding the new noises to the generated EIS data.
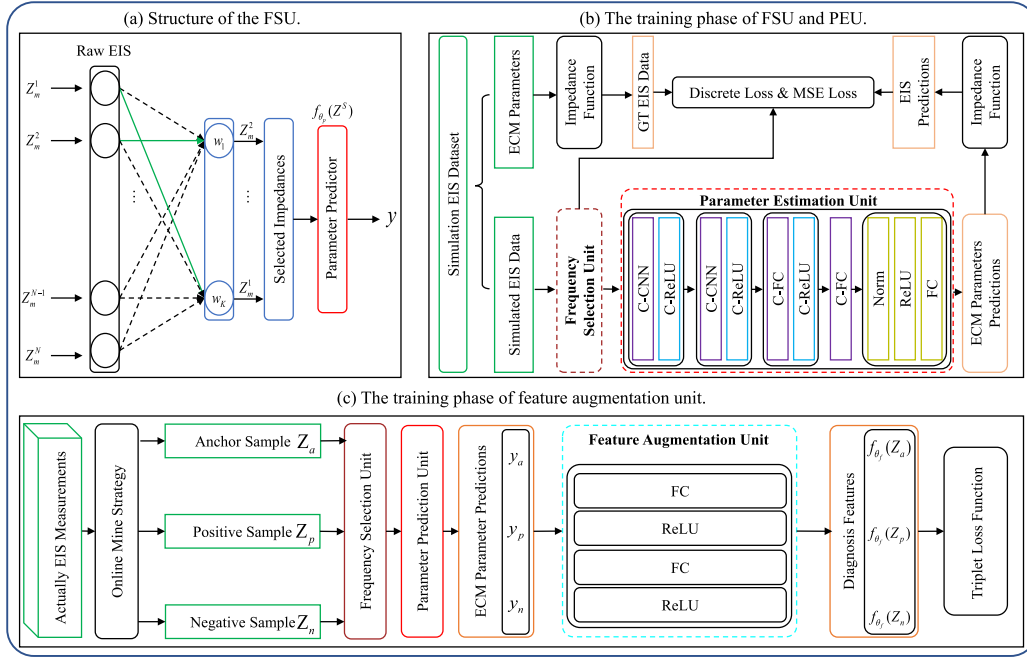
Fig. 3. The network structure of the proposed method.

In order to make the simulated EIS samples closely resemble real EIS data, it is necessary to incorporate prior knowledge to facilitate dataset generation [7,16]. The simulated ECM parameters should adhere to the coupling relationship between parameters and the external environment. Additionally, considering that the dominant factors contributing to EIS measurement noise vary at different test frequencies [5], the noise for each test frequency should be estimated individually.

2.3. EIS-based diagnosis method

2.3.1. Frequency selection unit

The problem of the frequency selection is defined as follows. Let $D = \{(Z_1, p_1), (Z_2, p_2), \ldots, (Z_M, p_M)\}$ be a dataset of M EIS samples, each $Z \in R^N$ is a group of EIS data containing N frequency points, and the p is the corresponding ECM parameter. Let S indicate a subset of K frequency points and $Z^S \in R^K$, the reduced EIS samples containing only K frequency points in S. Assume the proposed PEU is $f_{\theta_p}(Z^S)$, where the θ_p contains all the learnable parameters in networks. The goal of the PEU is to learn the optimal S^* and θ^* that satisfies:

$$S^*, \theta^* = \arg\min_{S,\theta} \mathcal{L}\left(f_{\theta_p}(Z^S), p\right) \tag{1}$$

Where the $\mathcal{L}(y, p)$ is the loss function between predictions y and groundtruth p.

Vanilla Gumbel-Softmax: To make FSU embedded into the neural network and trained jointly, the Gumbel-Softmax method, which is a continuous relaxation of a discrete one-hot vector, is utilized in this framework. The frequency selection operation could be expressed as $Z_i^S = W^\top Z_i$, each selection neuron in the FSU (see Fig. 3(a)) takes all frequency points as input and produces a single output point. The weights in kth selection neuron is a one-hot vector denoted as $w_k \in R^N$, which will be parameterized by a learnable vector $\alpha_k \in R^N$, the nth element in w_k is defined as follows [17]:

$$w_{kn} = \frac{\exp\left(\left(\log \alpha_{kn} + G_{kn}\right)/\beta\right)}{\sum_{j=1}^{N} \exp\left(\left(\log \alpha_{kj} + G_{kj}\right)/\beta\right)} \tag{2}$$

Where G_{kj} is independent and identically distributed samples from the Gumbel distribution, and $\beta \in (0, +\infty)$ is the temperature parameter of the concrete distribution, which is utilized to control the extent of

relaxation. During the training process, β is set to converge to 0 from a large value manually, which allows the network to fully explore the different combinations of frequency points, and when $\beta \to 0$, the w_k is a one-hot vector.

Discrete Loss Function: The vanilla Gumbel-Softmax method always leads to the selection of duplicate frequencies since the selection units operate independently and do not interact with other neurons. Originally, the Gumbel-Softmax method is proposed for dimensionality reduction in dense vision datasets [18], or feature selection in high-dimensional biological data [19], and the duplicate selection is acceptable in these tasks. However, in the case of PEMFC EIS frequency selection, the duplicate selection will lead to a waste of computational resources and may induce the network to obtain the local optimal solution. To this end, a discrete loss function is proposed to reduce the occurrence of duplicate selection. The distance between the weights vectors is utilized to metric the similarity of selection neurons, and the discrete loss function could be defined as follows:

$$W = \{w_1, w_2, \ldots, w_K\}^\top \tag{3}$$

$$D = \|W\|^2 + \left\|W^\top\right\|^2 - 2WW^\top \tag{4}$$

$$\mathcal{L}_d = max\{0, \tau - \min_{i \neq j}\{D_{(i,j)}\}\}, i = 1\cdots K, j = 1\cdots K \tag{5}$$

τ is the relaxation coefficient that slowly increases during the training process, which could prevent premature convergence of selection neurons.

2.3.2. Parameter estimation unit

The structure of the PEU is illustrated in Fig. 3(b). The PEU is responsible for extracting ECM parameters from EIS data. The complex neural networks [20] are employed to process EIS impedances consisting of complex numbers, and the impedance function of ECM is embedded into the networks to make the network outputs consistent with PEMFC knowledge. Traditional parameter identification methods typically involve iterative processes to obtain accurate model parameters, and the initial value selection significantly affects the estimation results. In contrast, the proposed PEU addresses these challenges and greatly improves computational efficiency, which enhances the usefulness of the proposed method.

Table 1
The basic parameters of investigated stack.

Parameter	Value
Anode Stoichiometry(H_2)	1.5
Cathode Stoichiometry (Air)	1.85
Electrode active surface	301 cm^2
Anode relative humidity	50%
Cathode relative humidity	41.92%
Pressure at H_2 inlet	250 KPa
Pressure at Air inlet	240 KPa
Temperature of the cooling circuit	74 °C
Coolant pressure	245 KPa
Fuel used during experiment	100% H_2
Nominal current density	1.0 A/cm^2
Number of cells	413

Table 2
The preset range of the investigated parameters.

CD (A/cm^2)	SC (-)	RH (%)	P (KPa)	T (° C)
0.2	1.9-3.8 (3.4)	20-100 (37.26)	108-160 (120)	30-80 (61)
0.3	1.4-3.0 (2.8)	20-100 (45.80)	113-165 (135)	30-80 (62)
0.6	1.2-2.3 (2.1)	20-100 (43.91)	152-210 (180)	30-80 (68)
1.0	1.3-2.1 (1.8)	20-100 (41.97)	212-270 (240)	30-80 (74)
1.5	1.4-2.0 (1.7)	20-100 (36.62)	227-270 (250)	35-80 (75)
1.6	1.4-2.0 (1.7)	20-100 (37.20)	227-270 (250)	35-80 (75)

(·) represents the nominal value of operating parameter.

The PEU and FSU will be jointly trained with a large-scale simulated EIS dataset, and the loss function of this step includes the MSE loss and the proposed discrete loss. Notice that the MSE loss is calculated from the predicted EIS and actual EIS, instead of directly constraining the error between the ECM parameter predictions. This makes the prediction loss independent of the parameter scale. The loss function of this training step could be represented as follows:

$$\mathcal{L}_1 = \mathcal{L}_{mse} + \lambda_1 \cdot \mathcal{L}_d \tag{6}$$

$$Z = \mathcal{F}_{imp}(y) = \{z^1, z^2, \ldots, z^N\} \tag{7}$$

$$\hat{Z} = \mathcal{F}_{imp}(p) = \{\hat{z}^1, \hat{z}^2, \ldots, \hat{z}^N\} \tag{8}$$

$$\mathcal{L}_{mse} = \frac{1}{N}\sum_{i=1}^{N}((\Re(z^i) - \Re(\hat{z}^i))^2 + (\Im(z^i) - \Im(\hat{z}^i))^2) \tag{9}$$

Where $\mathcal{F}_{imp}$ is the impedance function of ECM, y is the predicted ECM parameter and p is the groundtruth, the λ_1 is a hyperparameter for equalizing two losses.

2.3.3. Feature augmentation unit

The ECM parameters are susceptible to substantial variations stemming from normal operational [5,7,21], thereby impacting the robustness of the diagnosis framework. To this end, The FAU, which consists of a simple Multilayer Perceptron (MLP), is proposed to effectively transform ECM parameters into reliable diagnosis features. The structure of the FAU is depicted in Fig. 3(c). The FAU is trained using actual EIS measurements with the assistance of a triplet loss function [22]. Specifically, only the parameters of the FAU are updated at this stage. The triplet loss function is defined as follows:

$$\mathcal{L}_t = max(\left\|f_{\theta_f}(Z_a) - f_{\theta_f}(Z_p)\right\|^2 - \left\|f_{\theta_f}(Z_a) - f_{\theta_f}(Z_n)\right\|^2 + C, 0) \tag{10}$$

Where the C is a hyperparameter to control the minimum interval between different EIS fault samples, the f_{θ_f} is the proposed feature encoder. The triplets are obtained by online mine strategy in the mini-batch, and the Z_a, Z_p, and Z_n are the anchor data, positive data, and negative data, respectively. The L_2 regularization [23] is adopted in our framework, thus, the loss function of FAU is defined as follows:

$$\mathcal{L}_2 = \mathcal{L}_t + \lambda_2 \cdot \sum_{i=1}^{n} w_i^2 \tag{11}$$

Where the w_i are the parameters of the FAU, and λ_2 is a hyperparameter to control the extent of regularization.

3. Test bench and PEMFC properties

3.1. Experiment and test bench

This experiment focuses on the investigation of a commercial PEMFC stack designed for automotive applications. The basic parameters of the stack are outlined in Table 1. To elucidate the characteristics of the PEMFC under different operating conditions, various parameters such as current density (CD), operating temperature (T), gas pressure (P), relative humidity (RH), and cathode stoichiometry (SC) are carefully controlled and monitored using the Greenlight test station (G900), as shown in Fig. 4(a). These operating parameters are intentionally varied within predetermined ranges. The individual effect of each operating parameter on the FC is analyzed. In each case, only one parameter is changed, while the remaining parameters are maintained at their normal values. The predefined range for each operating parameter is detailed in Table 2.

The EIS works by analyzing the frequency response of the excitation signal at a specific frequency, which enables the assessment of the internal state of the PEMFC. An impedance spectrometer is used to acquire EIS (shown in Fig. 4(b)), and the test frequency of the excitation signal ranges from 0.01 Hz to 10 kHz in this experiment. The 101 test frequencies are selected, and the entire measurement process takes about 15 min to acquire a complete EIS. Therefore, the EIS measurement process is time-consuming, which poses a challenge to the practical usage of EIS-based models.

3.2. PEMFC performance evaluation

3.2.1. Influence of current density

The PEMFC is designed to operate at different current densities to accommodate load variations in real-world applications. In this study, the performance of the PEMFC under different current densities is investigated, as depicted in Fig. 5. As the current density rises, oxygen consumption progressively increases, resulting in increased water production. As more water is generated, the humidity within the PEMFC increases. This elevated moisture content plays a crucial role in diminishing membrane resistance, thereby facilitating the movement of protons across the membrane. Besides, heightened humidity contributes to a reduction in resistance at both the anode and cathode, as catalytic reactions are known to thrive in such environments. Nevertheless, the upsurge in humidity leads to heightened resistance for reactant gases attempting to access the reaction site, primarily due to the obstruction of porous material passages by water. Consequently, as the current density increases, charge transfer resistance and membrane resistance experience a decrease, while mass transfer resistance undergoes an increment.

However, it is important to note that these parameter changes occur during normal operation and do not signify faults. As a result, the reliable of ECM parameters for fault diagnosis is limited in this context.

3.2.2. Influence of different operation conditions

Fig. 6 displays the EIS curves obtained with various operating conditions. A decrease in SC leads to an increase in total impedance. Insufficient oxygen availability causes an elevation in charge transfer resistance and mass diffusion resistance, while the capacitance decreases due to inadequate air storage in the cathode (refer to Fig. 6(a)). RH directly affects the water content of the FC. The results depicted in Fig. 6(b) indicate that both excessively high and low RH levels contribute to an increase in total impedance, and these resistances exhibit sensitivity to RH variations. In general, higher gas pressure and
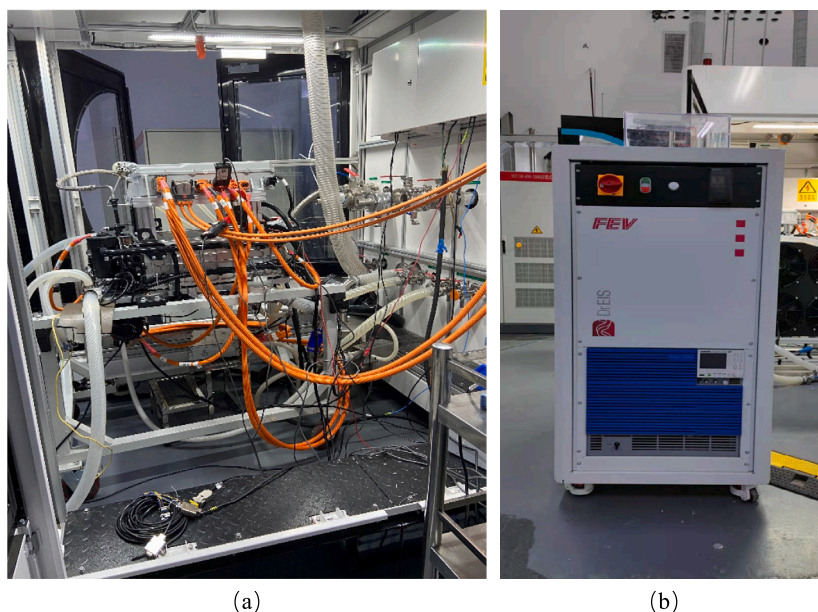
Fig. 4. The test bench of our experiments. The Fig. 4(a) is the G900 test station, and Fig. 4(b) is the impedance spectrometer.
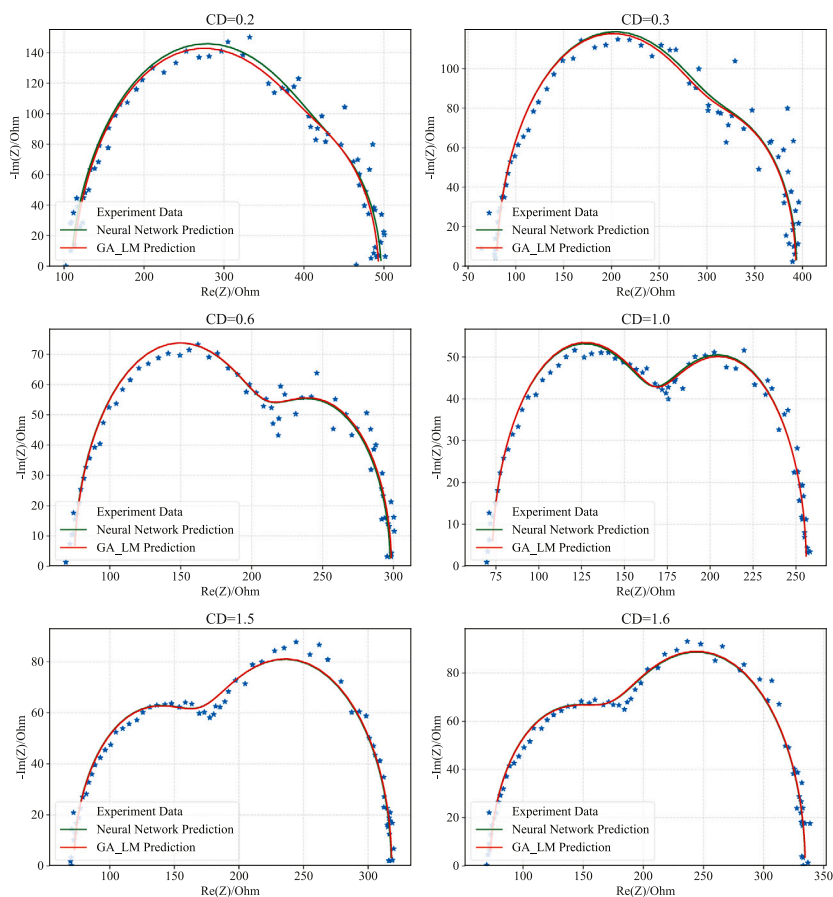

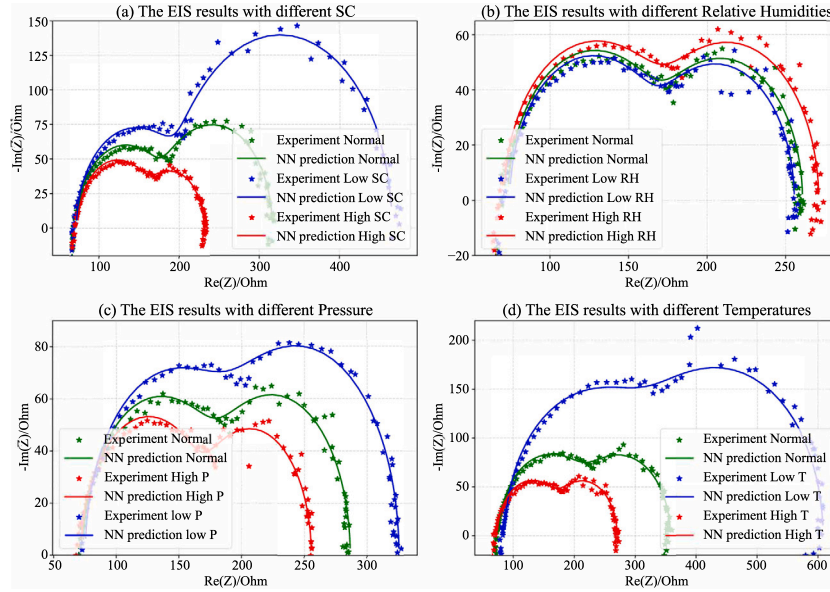**Fig. 5.** The EIS results with different current densities.

Fig. 6. The EIS results with different operation conditions.

operating temperature enhance the electrochemical reaction within the PEMFC, leading to lower impedance (refer to Fig. 6(c) (d)). However, operating at high temperatures and pressure also requires additional energy, and therefore the appropriate reaction environment should be selected to ensure economic efficiency.

4. Fault diagnosis experiments

4.1. Experiment details

4.1.1. Equivalent circuit model

It is crucial to select a suitable ECM for analyzing the EIS data in our experiments. The Randles ECM [24] is commonly employed to approximate the behavior of the PEMFC system. However, the complex representation of the Warburg impedance makes it difficult to insert the corresponding impedance function into the PEU for joint training, so it is necessary to replace the Warburg impedance in the Randles ECM with an RC circuit [25]. The impedance function of ECM in our experiment could be expressed as:

$$Z = R_m + \cfrac{1}{Q(jw)^n + \cfrac{1}{R_p + \cfrac{1}{j\omega C_w + \frac{1}{R_w}}}} \tag{12}$$

$$Z_{CPE} = \frac{1}{Q(jw)^n} = Z_0 w^{-n}(\cos\frac{n}{2}\pi - j\sin\frac{n}{2}\pi) \tag{13}$$

4.1.2. EIS dataset

The fault type of each EIS data is determined based on prior knowledge of the EIS plot and the observed behavior of the stack during the experiment. In general, when the flooding fault occurs, the FC cathode encounters compromised air ingress, resulting in an increased mass transfer resistance. This could be observed in the EIS plot as a gradual increase of the low-frequency arc. Additionally, in the case of a membrane drying fault, an insufficient water content within the electrolyte obstructs efficient proton conduction. During such instances, a notable manifestation is the heightened membrane resistance, specifically observable as an increase in resistance at high frequencies when the imaginary part is 0 in EIS plot.

In our experiments, a total of 310 groups of EIS data are collected under different operating parameters. Among these EIS data, 74 are classified as flooding faults, 69 are classified as membrane drying faults, and the remaining data are normal samples. These actual EIS

data are used to guide the generation of the large-scale simulated EIS dataset, and a total of 100,000 groups of simulated EIS data are generated. These generated EIS data are used to train the FSU and PEU, while the performance of the PEU is evaluated using the actual EIS measurements.

The FAU is trained by actual EIS data only with the contrastive learning paradigm, which could fully explore the characteristics of the EIS data, as well as realize the function of data augmentation. Half of the measured EIS data is used for FAU training, while the remaining EIS data is utilized to evaluate the performance of fault diagnosis. The training and testing datasets are divided using a stratified sampling strategy. This ensures the proportion of fault samples in each dataset is uniform, which is crucial for maintaining the integrity and reliability of the training process.

4.1.3. Evaluation metrics

The performance of ECM parameter estimation methods is evaluated using two metrics: Root Mean Square Error (RMSE) and Mean Absolute Error (MAE). These metrics quantify the errors between the predicted EIS data and the actual EIS measurements in our experiments. Besides, the fault diagnosis performance of PEMFC is assessed using Weighted Macro metrics, which encompass Accuracy, Precision, Recall, and F1-Score. These metrics provide a comprehensive evaluation of the diagnosis capabilities of our approach. In addition, the effectiveness of the frequency selection methods is measured based on the fault diagnosis performance. The 90% fault classification accuracy is taken as the benchmark, and a more effective frequency selection solution will require fewer frequency points to achieve the desired 90% classification accuracy.

4.2. Investigation of FSU and PEU

In this experiment, the effectiveness of the FSU will be investigated. The proposed method will be compared with the traditional parameter identification method GA-LM [7], where the initial value of Levenberg–Marquardt (LM) is generated based on fitting results of genetic algorithm (GA). The frequency selection solution of GA-LM are generated using uniform selection strategies and will serve as the baseline for comparison with the proposed frequency selection method. The experiment consists of four cases:
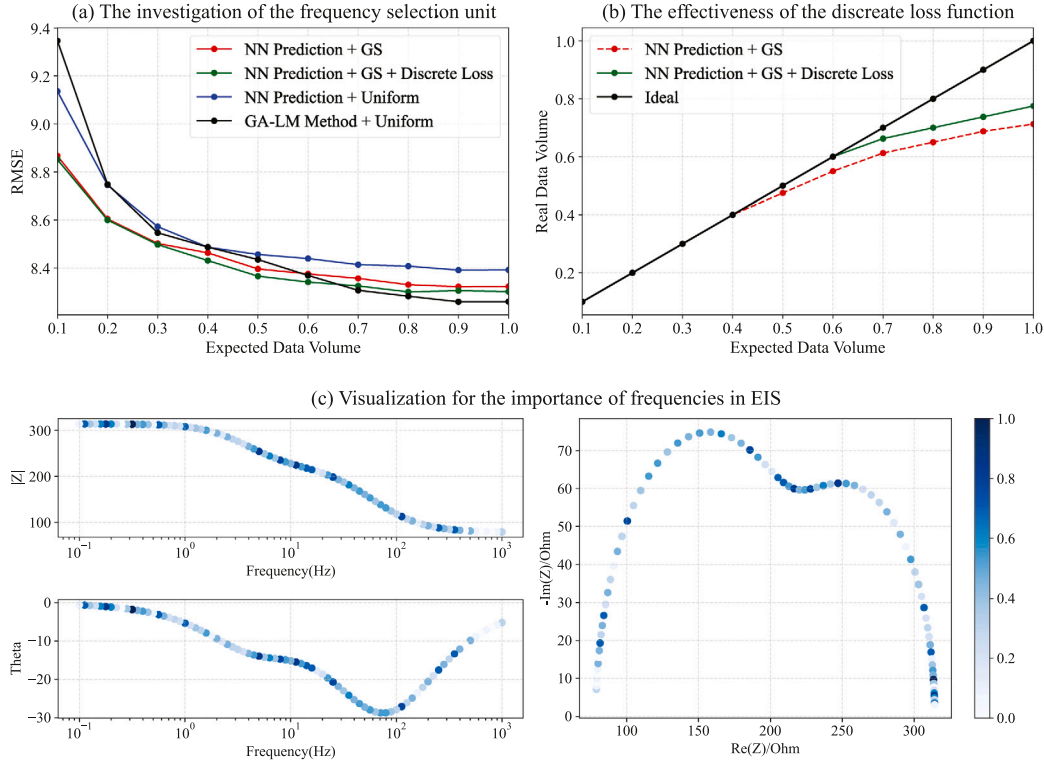
Fig. 7. The investigation of FSU and PEU.

1. Case 1: Predict the ECM parameters by the PEU, and the frequency selection solution is obtained by vanilla Gumbel-Softmax (GS) trick. (NN Prediction + GS)
2. Case 2: Predict the ECM parameters by the PEU, and obtain the frequency selection solution by GS trick which is trained by the proposed discrete loss function. (NN Prediction + GS + Discrete Loss)
3. Case 3: Predict the ECM parameters by the PEU, and generate the frequency selection solution by the uniform selection strategy. (NN Prediction + Uniform)
4. Case 4: The baseline method estimates the ECM parameters by GA-LM algorithm, and generates the frequency selection solution by uniform selection strategy. (GA-LM Method + Uniform)

The results of the four cases are presented in Fig. 7(a). The PEU has comparable prediction accuracy over the optimization-based method when the quantity of the selected frequency points was greater than 70%, which demonstrates the effectiveness of the PEU. Moreover, when the quantity of selected frequency points was less than 70%, the performance of the PEU outperforms the optimization-based method. The deep learning models could mine more useful prior knowledge from the training dataset to support the accurate prediction of ECM parameters with fewer selection frequency points. This advantage will facilitate the practical application of the proposed method.

On the other hand, the difference between Case 1, Case 2, and Case 3 demonstrate that the frequency selection solution has a significant impact on the accuracy of the prediction. The comparison between Case 1 and Case 2 illustrates the effectiveness of the proposed discrete loss function in steering the PEU away from local optimal solutions and making full use of computational resources, and Fig. 7(b) demonstrate that the proposed method could reduce the occurrence of the duplicate selection.

Finally, the amount of expected data volume is gradually increased under the conditions of Case 2, and the selection times of each frequency point are counted, the statistics are normalized and visualized

in Fig. 7(c). Darker colors indicate that the corresponding points are always selected, thus, these points are more important for the estimation of ECM parameters. Notably, most of the important frequency points selected by the neural network are located at the vertices and inflection points of the EIS Nyquist plot, which is consistent with the intuitive analysis of the PEMFC system.

4.3. Fault diagnosis performance

The FAU generates diagnosis features from the predicted ECM parameters and output fault diagnosis results with a simple classifier. In this experiment, effectiveness of FAU is evaluated first, and then present fault diagnosis results without the frequency selection method. Finally, fault diagnosis results combined with frequency selection solutions are generated in an end-to-end manner.

4.3.1. Investigation of the FAU

ECM parameters are easily influenced by routine operation and changes in the external environment, which can significantly affect the diagnosis performance. To address this limitation, a FAU is proposed to enhance the robustness of diagnosis features and improve the generalization of the EIS-based fault diagnosis framework. The diagnosis features are visualized by the T-SNE [26] algorithm, as shown in Fig. 8. It is clear that the proposed algorithm could aggregate the diagnosis features according to the PEMFC faults rather than operation conditions.

4.3.2. Fault diagnosis without frequency selection

In this experiment, various commonly used classifiers such as K-Nearest Neighbor (KNN), Decision Tree (DT), Random Forest (RF), Support Vector Machine (SVM), Logistic Regression (LR) and Naive Bayes are employed to generate fault diagnosis results. The performance of the proposed method is compared with the traditional framework, where the proposed method uses the PEU to predict the ECM parameters and the FAU is used to obtain the diagnosis features. In
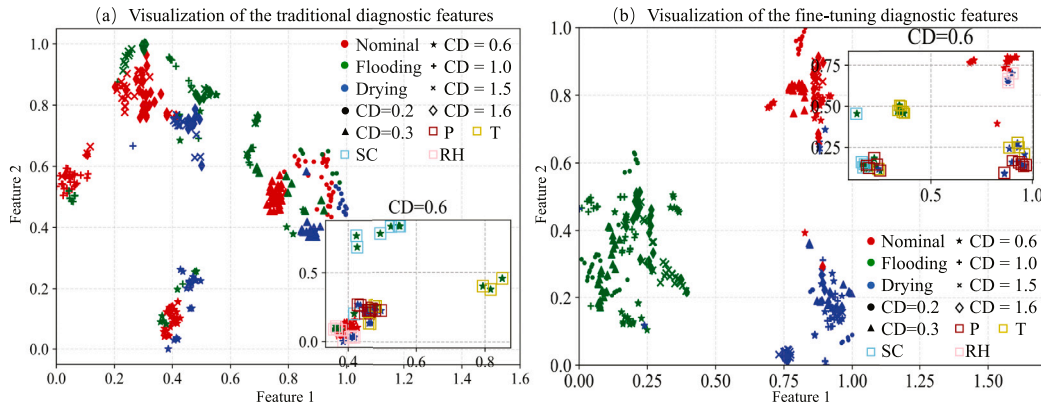
Fig. 8. Visualization of the diagnosis features.

Table 3
Fault diagnosis performance without frequency selection.

Classifiers	Traditional diagnosis framework				Proposed diagnosis method			
	Accuracy	Precision	Recall	F1-Score	Accuracy	Precision	Recall	F1-Score
KNN	0.8704	**0.9052**	0.6417	**0.7141**	0.9167	0.9150	0.8905	0.8584
DT	**0.8796**	0.7739	**0.6708**	0.6901	0.8981	0.9121	0.8536	0.8425
RF	0.8796	0.7265	0.6333	0.6420	0.9167	0.9179	**0.8905**	0.8399
LR	0.7685	0.5873	0.3833	0.3752	0.9032	0.8813	0.8515	0.8655
Naive Bayes	0.7407	0.5921	0.5083	0.5229	0.8774	0.8545	0.8589	0.8552
SVM (linear)	0.7685	0.5873	0.3833	0.3752	**0.9352**	**0.9187**	0.8583	**0.8890**
SVM (poly)	0.8426	0.8059	0.6042	0.6646	0.9259	0.9092	0.8542	0.8706
SVM (rbf)	0.8241	0.9017	0.5083	0.5576	0.9167	0.9004	0.8125	0.8605

contrast, the traditional method utilizes an optimization-based method to identify the model parameters, which will be used as the inputs of fault classifiers. It should be noted that all frequency points are used to predict the ECM parameters in this experiment. The comparison results of the two diagnosis methods are shown in Table 3.

The results in Table 3 show that the proposed framework outperforms the traditional methods significantly in terms of fault diagnosis performance, which is attributed to the robust diagnosis features generated by the proposed FAU. In fact, ECM parameters may not be sufficient for the development of a general fault diagnosis framework, an effective feature augmentation method is crucial to ensure the versatility and effectiveness of the fault diagnosis framework.

4.3.3. End-to-end fault diagnosis results

In this experiment, the frequency selection solution is combined with the fault diagnosis algorithm to provide the end-to-end diagnosis results. Specifically, the proposed method, which obtain the ECM parameters by PEU, will compare with the traditional paradigm, which estimate the ECM parameters with optimization method. The parameters generated by both algorithms are then processed by our proposed FAU simultaneously. The diagnosis results are generated by SVM classifier, which obtain the best performance in the preview experiment. The fault diagnosis performance with different data volume are compared in Table 4. As shown in the Table 4, the fault diagnosis performance gradually improves with an increase in the number of measured frequency points, which is consistent with intuition. Moreover, our proposed algorithm achieved 90% diagnosis accuracy when the input data volume was only 40% of the total frequency points, while the optimization-based algorithm required 60% of the total number of frequency points to achieve the same measurement accuracy. This result indicates that our proposed algorithm can reduce the number of frequency points that need to be measured while ensuring prediction accuracy.

Table 4
End-to-end PEMFC fault diagnosis performance. The *S.P.* represents the data volume actually selected by the frequency selection algorithm.

Expected	Accuracy	Precision	Recall	F1-Score	S.P.
Data volume	Proposed diagnosis method				
1.0	0.943	0.932	0.927	0.928	0.78
0.9	0.941	0.930	0.909	0.924	0.74
0.8	0.938	0.929	0.924	0.921	0.70
0.7	0.932	0.925	0.917	0.914	0.66
0.6	0.922	0.912	0.890	0.908	0.60
0.5	0.911	0.903	0.879	0.896	0.50
0.4	**0.901**	**0.895**	**0.863**	**0.884**	**0.40**
0.3	0.879	0.878	0.846	0.862	0.30
0.2	0.866	0.867	0.828	0.850	0.20
0.1	0.848	0.850	0.810	0.825	0.10
	Traditional diagnosis method				
1.0	0.944	0.933	0.915	0.923	1.00
0.9	0.943	0.932	0.913	0.924	0.90
0.8	0.935	0.920	0.899	0.914	0.80
0.7	0.930	0.905	0.887	0.894	0.70
0.6	**0.912**	**0.895**	**0.880**	**0.884**	**0.60**
0.5	0.891	0.884	0.875	0.876	0.50
0.4	0.878	0.874	0.868	0.879	0.40
0.3	0.864	0.849	0.871	0.833	0.30
0.2	0.857	0.794	0.850	0.833	0.20
0.1	0.802	0.740	0.801	0.766	0.10

5. Conclusion

In this paper, a novel EIS-based diagnosis framework along with a frequency selection method for PEMFC are proposed. Our proposed approach includes a deep learning-based PEU that directly predicts ECM parameters from EIS data. The FSU is designed with a Gumbel-Softmax trick to parameterize the effect of frequency points in EIS for fault diagnosis, which enables us to obtain the optimal frequency

selection solution. A discrete loss function is proposed to train the selection neurons in the FSU, avoiding the duplicate selection of frequency points. Furthermore, to improve the versatility of EIS-based fault diagnosis framework, the FAU is introduced to generate reliable features for fault diagnosis. This enables the proposed method to be effectively applied in diverse working environments. Finally, a simple classifier is employed to generate diagnosis results with the features generated by FAU. The performance of our proposed framework is evaluated with EIS data acquired from a commercial PEMFC stack. The experimental results demonstrate that our approach surpasses traditional frameworks in terms of efficiency and accuracy, highlighting its potential for real-world applications.

Declaration of competing interest

The author(s) declared no potential conflicts of interest with respect to the research, authorship, and/or publication of this article.

Data availability

The authors do not have permission to share data.

References

[1] J. Wang, B. Yang, C. Zeng, Y. Chen, Z. Guo, D. Li, H. Ye, R. Shao, H. Shu, T. Yu, Recent advances and summarization of fault diagnosis techniques for proton exchange membrane fuel cell systems: A critical overview, J. Power Sources 500 (2021) 229932.

[2] J. Li, C. Yan, Q. Yang, D. Hao, W. Zou, L. Gao, X. Zhao, Quantitative diagnosis of PEMFC membrane humidity with a vector-distance based characteristic mapping approach, Appl. Energy 335 (2023) 120610.

[3] B. Zuo, Z. Zhang, J. Cheng, W. Huo, Z. Zhong, M. Wang, Data-driven flooding fault diagnosis method for proton-exchange membrane fuel cells using deep learning technologies, Energy Convers. Manage. 251 (2022) 115004.

[4] Z. Tang, Q.-A. Huang, Y.-J. Wang, F. Zhang, W. Li, A. Li, L. Zhang, J. Zhang, Recent progress in the use of electrochemical impedance spectroscopy for the measurement, monitoring, diagnosis and optimization of proton exchange membrane fuel cell performance, J. Power Sources 468 (2020) 228361.

[5] H. Lu, J. Chen, C. Yan, H. Liu, On-line fault diagnosis for proton exchange membrane fuel cells based on a fast electrochemical impedance spectroscopy measurement, J. Power Sources (2019).

[6] S. Laribi, K. Mammar, Y. Sahli, K. Koussa, Analysis and diagnosis of PEM fuel cell failure modes (flooding & drying) across the physical parameters of electrochemical impedance model: Using neural networks method, Sustain. Energy Technol. Assess. 34 (2019).

[7] Y. Ao, S. Laghrouche, D. Depernet, Diagnosis of proton exchange membrane fuel cell system based on adaptive neural fuzzy inference system and electrochemical impedance spectroscopy, Energy Convers. Manage. 256 (2022) 115391.

[8] A. Debenjak, J. Petrov, P. Bokoski, B. Musizza, J. Jurii, Fuel cell condition monitoring system based on interconnected DC–DC converter and voltage monitor, IEEE Trans. Ind. Electron. 62 (8) (2015) 5293–5305.

[9] N. Katayama, S. Kogoshi, Real-time electrochemical impedance diagnosis for fuel cells using a DC-DC converter, IEEE Trans. Energy Convers. 30 (2) (2014) 707–713.

[10] P. Hong, L. Xu, H. Jiang, J. Li, M. Ouyang, A new approach to online AC impedance measurement at high frequency of PEM fuel cell stack, Int. J. Hydrogen Energy 42 (30) (2017) 19156–19169.

[11] F. Xiao, T. Chen, Y. Peng, R. Zhang, Fault diagnosis method for proton exchange membrane fuel cells based on EIS measurement optimization, Fuel Cells 22 (4) (2022) 140–152.

[12] B. Najafi, P. Bonomi, A. Casalegno, F. Rinaldi, A. Baricci, Rapid fault diagnosis of PEM fuel cells through optimal electrochemical impedance spectroscopy tests, Energies 13 (14) (2020) 3643.

[13] T. Ma, Z. Zhang, W. Lin, J. Kang, Y. Yang, Development of Online Fault Diagnosis Method for PEM Fuel Cell Based on Impedance at Optimal Frequency, Technical Report, SAE Technical Paper, 2020.

[14] E. Jang, S. Gu, B. Poole, Categorical reparameterization with gumbel-softmax, 2016, arXiv preprint arXiv:1611.01144.

[15] Y. Chen, D. Zhang, Integration of knowledge and data in machine learning, 2022, arXiv preprint arXiv:2202.10337.

[16] S. Laghrouche, J. Liu, F.S. Ahmed, M. Harmouche, M. Wack, Adaptive second-order sliding mode observer-based fault reconstruction for PEM fuel cell air-feed system, IEEE Trans. Control Syst. Technol. 23 (3) (2014) 1098–1109.

[17] C.J. Maddison, A. Mnih, Y.W. Teh, The concrete distribution: A continuous relaxation of discrete random variables, 2016, arXiv preprint arXiv:1611.00712.

[18] A. Abid, M.F. Balin, J. Zou, Concrete autoencoders for differentiable feature selection and reconstruction, 2019, arXiv preprint arXiv:1901.09346.

[19] D. Singh, H. Climente-González, M. Petrovich, E. Kawakami, M. Yamada, Fsnet: Feature selection network on high-dimensional biological data, 2020, arXiv preprint arXiv:2001.08322.

[20] C. Trabelsi, O. Bilaniuk, D. Serdyuk, S. Subramanian, J.F. Santos, S. Mehri, N. Rostamzadeh, Y. Bengio, C.J. Pal, Deep complex networks, CoRR abs/1705.09792, 2017, arXiv:1705.09792.

[21] J. Lv, J. Kuang, Z. Yu, G. Sun, J. Liu, J.I. Leon, Diagnosis of PEM fuel cell system based on electrochemical impedance spectroscopy and deep learning method, IEEE Trans. Ind. Electron. (2023).

[22] F. Schroff, D. Kalenichenko, J. Philbin, Facenet: A unified embedding for face recognition and clustering, in: Proceedings of the IEEE Conference on Computer Vision and Pattern Recognition, 2015.

[23] I. Goodfellow, Y. Bengio, A. Courville, Deep Learning, MIT Press, 2016.

[24] J.E.B. Randles, Kinetics of rapid electrode reactions, Discuss. Faraday Soc. 1 (1947) 11–19.

[25] P. Pathapati, X. Xue, J. Tang, A new dynamic model for predicting transient phenomena in a PEM fuel cell system, Renew. Energy (2005).

[26] L. Van der Maaten, G. Hinton, Visualizing data using t-SNE, J. Mach. Learn. Res. 9 (11) (2008).